Review of Palaeobotany and Palynology 168 (2011) 21–30

Contents lists available at SciVerse ScienceDirect

Review of Palaeobotany and Palynology

journal homepage: www.elsevier.com/locate/revpalbo

Research paper

Holocene coastal vegetation changes at the mouth of the Amazon River

Clarisse Beltrão Smith [a], Marcelo Cancela Lisboa Cohen [a,b,*], Luiz Carlos Ruiz Pessenda [c], Marlon Carlos França [a], José Tasso Felix Guimarães [a], Dilce de Fátima Rossetti [d], Rubén José Lara [e]

[a] Post-Graduate Program in Geology and Geochemistry, Coastal Dynamics Laboratory, Federal University of Pará, Avenida Perimentral 2651, Terra Firme, CEP: 66077-530, Belém (PA), Brazil
[b] Faculty of Oceanography, Federal University of Pará, Rua Augusto Corrêa 1, Guama, CEP: 66075-110, Belém (PA), Brazil
[c] São Paulo University, ^{14}C Laboratory, Avenida Centenário 303, 13416000 Piracicaba, SP, Brazil
[d] National Space Research Institute (INPE), Rua dos Astronautas 1758-CP 515, CEP: 12245-970, São José dos Campos (SP), Brazil
[e] Center for Tropical Marine Ecology (ZMT), Fahrenheitstr. 6, 28359 Bremen, Germany

ARTICLE INFO

Article history:
Received 8 March 2011
Received in revised form 19 September 2011
Accepted 21 September 2011
Available online 29 September 2011

Keywords:
Amazon region
climatic change
herbaceous vegetation
mangrove
palynology

ABSTRACT

Wetland dynamics in the eastern Amazon region during the past 7000 years were studied using pollen, textural and structural analyses of sediment cores, as well as AMS radiocarbon dating. Four sediment cores were sampled from Marajó Island, which is located at the mouth of the Amazon River. Marajó Island is covered mainly by Amazon coastal forest, as well as herbaceous and *varzea* vegetation. Three cores were sampled from Lake Arari, which is surrounded by herbaceous vegetation flooded by freshwater. One core was sampled from a herbaceous plain located 15 km southeast of Lake Arari. Pollen preservation in the sedimentary deposits from this lake and from its drainage basin suggests significant vegetation changes on Marajó Island during the mid- and late-Holocene. Between 7328–7168 and 2306–2234 cal. yr BP, mangrove vegetation was more widely distributed on the island than it is today. During the past 2306–2234 cal. yr BP herbaceous vegetation expanded. Sedimentary structures and pollen data suggest a lagoon system until ~2300 cal. yr BP. The current distribution of mangroves along the Pará littoral, together with the presence of mangrove pollen and the sedimentary structures of the cores, indicates greater marine influence during the mid-Holocene. This may be attributed to the association between the eustatic sea-level change and the dry period recorded in Amazonia during the early- and mid-Holocene, followed by a wet phase over the past 2000 years.

1. Introduction

The littoral of Marajó Island, at the mouth of the Amazon River, is part of the longest mud coastline in the world with ca. 13,800 km^2 (Kjerfve and Lacerda, 1993). The nature of this coastal marine mud reflects climatic changes in the Amazon basin (Pujos et al., 1996), and the mangroves which colonize this littoral are considered to be highly susceptible to climatic change (e.g., Alongi, 2008; Cohen et al., 2008, 2009; Lara and Cohen, 2009; Versteegh et al., 2004) as it impacts multiple ecological factors such as salinity, nutrients, input of fresh water, and sea-level changes (Krauss et al., 2008; Stevens et al., 2006; Stuart et al., 2007). Generally, these parameters are related to sea-level oscillations due to climatic fluctuations, although tectonics might have played a role in this geological setting (e.g., Miranda et al., 2009; Rossetti et al., 2007a).

Regarding the hinterland of the Amazon region, several studies indicate that during the early- and mid-Holocene savanna vegetation expanded, likely reflecting a drier climate (e.g., Behling and Hooghiemstra, 2000; Freitas, et al., 2001; Pessenda et al., 2004). During the late-Holocene arboreal vegetation became more prominent in the Amazon basin due to the return of more humid climate conditions, likely similar to the present day. However, recent research indicates that vegetation changes in the Amazon region may have been caused by tectonic events (e.g., Rossetti and Valeriano, 2007; Rossetti et al., 2007a, 2008, 2010).

In terms of vegetation changes caused by climatic fluctuations, rainfall variations in the Amazonian hydrographic region likely controlled the volume of the Amazon River which displays the world's greatest water discharge with 6300 km^3 yr^{-1} (Eisma et al., 1991). Consequently, during the dry period of the early- and mid-Holocene the Amazon River's inflow may have been severely reduced (Amarasekera et al., 1997; Toledo and Bush, 2007, 2008), similar to the Younger Dryas event, when river discharge was reduced by at least 40% relative to present conditions (Maslin and Burns, 2000). Thus, significant changes in river water discharge along the littoral would be expected, and this would have affected salinity gradients along the coastline of Marajó Island. This process would drive changes in the distribution of mangrove (brackish water vegetation)

* Corresponding author at: Post-Graduate Program in Geology and Geochemistry, Coastal Dynamics Laboratory, Federal University of Pará, Avenida Perimentral 2651, Terra Firme, CEP: 66077-530, Belém (PA), Brazil.
E-mail address: mcohen@ufpa.br (M.C.L. Cohen).

0034-6667/$ – see front matter © 2011 Elsevier B.V. All rights reserved.
doi:10.1016/j.revpalbo.2011.09.008

and varzea/herbaceous vegetation (freshwater vegetation) on Marajó Island.

Mangroves have undergone almost continuous disturbance as a result of fluctuations in sea-level over the past 11,000 years (Behling et al., 2001a; Blasco et al., 1996; Cohen et al., 2008; Hait and Behling, 2009). The rapid rise in global sea-level during the early Holocene is mainly attributed to climatically controlled glacio-eustatic factors (e.g., Fairbridge, 1962). Over the past 5000 years in the northern Brazilian littoral, very little change in relative sea-level has been observed (e.g., Behling et al., 2001a; Cohen et al., 2005a, 2005b; Vedel et al., 2006). In fact, during the late Holocene local and regional controlling factors become more perceptible. Forces such as precipitation, which strongly influences run-off and river discharge, can result in local "eustatic" sea-level variations (e.g., Mörner, 1996) and significant salinity gradient changes along estuaries (e.g., Lara and Cohen, 2006).

Vegetation history during the late Holocene along the littoral of northern Brazil is characterized by mangrove expansion/contraction phases (e.g., Behling et al., 2001a; Cohen et al., 2005a, 2005b; Cohen et al., 2008, 2009). These phases have been interpreted as changes in the relative sea-level and/or river water discharge, since the current distribution of mangrove on this littoral is mainly controlled by fresh water discharge and substratum topography (Cohen and Lara, 2003; Cohen et al., 2005a, 2005b, 2008, 2009; Lara and Cohen, 2006, 2009).

Alternatively, under the tectonic hypothesis to explain vegetation changes in the hinterland, the water discharge of the Amazon River could not have been significantly affected. This follows from the fact that tectonic activity during the Quaternary may have affected the channel network (e.g. Martelli et al., 2009) while the river water volume is controlled by rainfall (Marengo et al., in press). Consequently, considering only tectonic influences, no relationship between vegetation changes in the Amazon region and wetland dynamics on the littoral are expected.

Here we present pollen data, facies descriptions of sediment cores, and AMS radiocarbon dating of lacustrine deposits located in the mouth of the Amazon River. The aim is to contribute additional data to the understanding of wetland dynamics at the mouth of the Amazon, and to discuss different hypotheses related to vegetation changes in the Amazon Region during the Holocene either as a consequence of climatic alterations (e.g., Behling and Hooghiemstra, 2000; Freitas, et al., 2001; Pessenda et al., 2004) or tectonism (e.g., Rossetti et al., 2007a, 2008).

2. Study area

2.1. Location

The study site is located on Marajó Island, in northeastern Amazonia (Fig. 1). This island is found at the mouth of the Amazon River in the state of Pará, Brazil. Samples were collected in Lake Arari, which is a N–S elongated feature with a depth of approximately 2–4 m and an area of ~100 km^2. The lake is located in the central-eastern part of Marajó Island, ~70 km from the modern coastline. To the north, it connects to the Atlantic Ocean by the Tartarugas channel which was artificially enlarged. To the south, it forms the headwaters of the Arari River, which runs southeast and drains into Marajó Bay (Fig. 1).

2.2. Geological, physiographical and hydrographical setting

Marajó Island is formed by sandstones and mudstones of the Barreiras Formation, followed by post-Barreiras deposits which rapidly become thicker westwards in the sub-surface, reaching up to 120 m in the Lake Arari area (Rossetti et al., 2008). This area is dominated by Quaternary deposits related to the latest deposition phase of the Tucunaré–Pirarucu succession (see Rossetti et al., 2007b).

The eastern part of Marajó Island is mostly characterized by lowlands with altitudes averaging only 4–6 m above modern sea-level

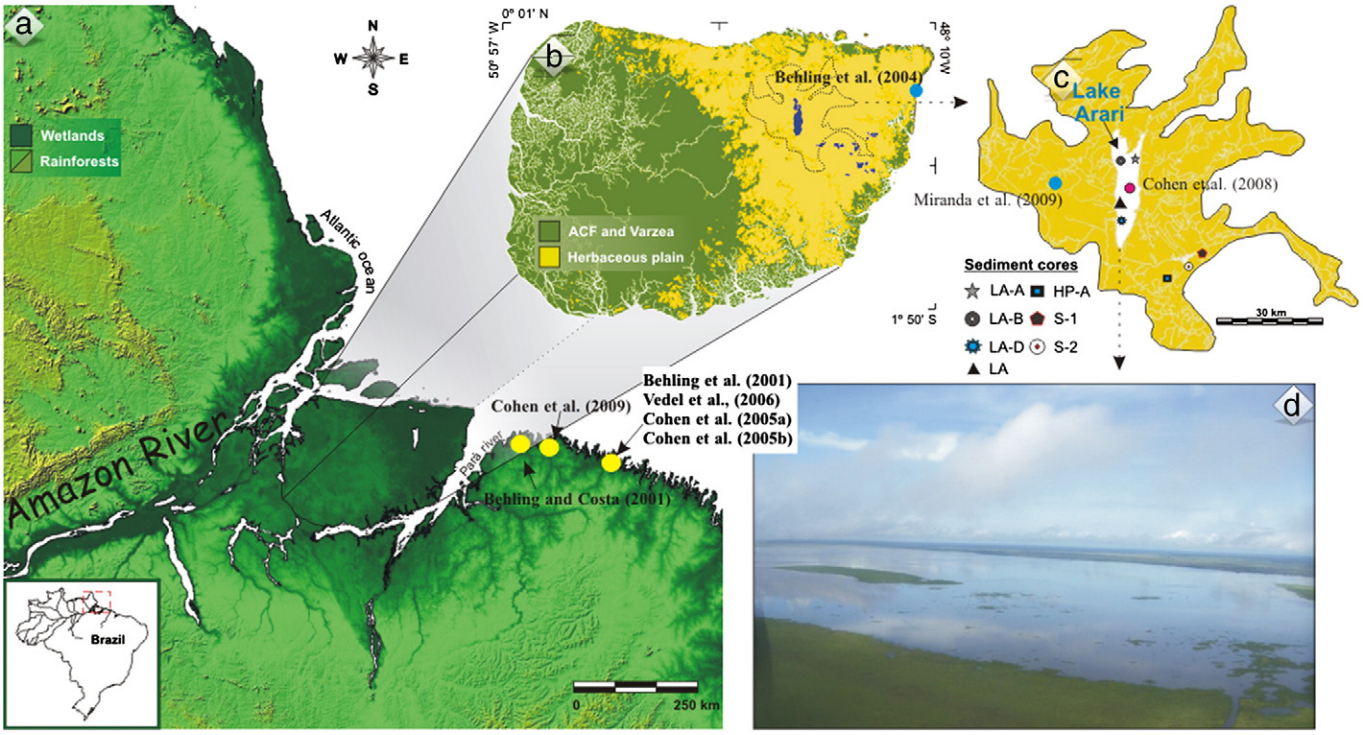

Fig. 1. Sediment core location and the distribution of main vegetation units on Marajó Island after Cohen et al. (2008). Aerial photo of Lake Arari. LA, S-1 and S-2 cores (Cohen et al., 2008).

(Rossetti et al., 2007a, 2008), and is dominated by Holocene sedimentation (Behling et al., 2004) which is slightly depressed relative to the western side (Behling et al., 2004; Lara and Cohen, 2009; Rossetti et al., 2007a).

The drainage basin area of Lake Arari consists of a series of dendritic and anastomosing channels (Cohen et al., 2008) that are superimposed on a palimpsest drainage system (Rossetti et al., 2007a). A large channelized funnel-shaped morphology – related to the paleoestuarine system, a network of paleochannels and sandy bars – is observed in the area surrounding Lake Arari (Rossetti et al., 2007b, 2008).

2.3. Present climate and vegetation

The region is characterized by a tropical warm and humid climate with annual precipitation ~2680 mm and a mean annual temperature of 27 °C. A drier period of lower rainfall occurs between July and December and a rainy season occurs between January and June, with monthly rainfall averaging 87 and 340 mm, respectively (IDESP, 1974).

The lake suffers a reduction in area of approximately 80% during the dry season, because it is mainly rainfed. Water salinity is 0 and the pH ranges between 6 and 8.2. Mean water temperature is 27 °C, and dissolved oxygen contents between 3.3 and 5.5 mg/L were measured in May 2009.

In contrast to most regions of Amazonia, where dense forest dominates, northeastern Marajó Island consists of open vegetation. *Restinga* vegetation is represented by shrubs and herbs (e.g., *Anacardium*, *Byrsonima*, *Annona*, *Acacia*) that occur on sand plains and dunes near the shoreline. This vegetation unit and mangrove, represented by *Rhizophora* and *Avicennia*, occur in such small areas along the littoral of this island that it was not possible to show them on the map (Fig. 1). Vegetation around the lake consists of natural open areas dominated by Cyperaceae and Poaceae that widely colonize the eastern side of the island of Marajó, while *várzea* vegetation (composed of wetland trees such as *Euterpe oleracea* (açai) and *Hevea guianensis* (rubber tree)) and "Terra Firme" vegetation (composed of terrestrial trees such as *Cedrela odorata* (cedar), *Hymenaea courbaril* (Jatoba) and *Manilkara huberi* (Maçaranduba) occur on the western side (Cohen et al., 2008). Narrow and elongated belts of dense ombrophilous forest are also present along riverbanks (Rossetti et al., 2008).

2.4. Mangrove development on the littoral of northern Brazil

Wetlands occur within specific topographic zone (see Cohen and Lara, 2003; Cohen et al., 2005a, 2005b, 2008, 2009; Furukawa and Wolanski, 1996) depending on physical (sediment type, e.g., Duke et al., 1998) and chemical (nutrient availability and sediment salt concentrations across the intertidal area, Hutchings and Saenger, 1987; Wolanski et al., 1990) characteristics.

In the littoral of northern Brazil, the surface salinity distribution pattern reflects the northwestward movement of waters from the Amazon and Pará Rivers pushed by the North Brazil Current (Santos et al., 2008). Mangroves are distributed within specific topographic and salinity ranges (Cohen et al., 2005a), where pore water salinity is between 30 and 85‰ (Lara and Cohen, 2006).

Mangroves tolerant higher soil salinity than *várzea* vegetation (Gonçalves-Alvim et al., 2001), and the majority of the Marajó Island coastline is currently inundated by freshwater river inflows. Thus a maximum pore water salinity of approximately 5‰ is recorded in the transition zone, which is mainly colonized by *Rhizophora* (mangrove) and Arecaceae (várzea) and located on the island's northeastern coastline (see Cohen et al., 2008, Fig. 1). Interstitial salinity is zero in sediments colonized by herbaceous and *várzea* vegetation in the coastline and interior of Marajó Island.

Considering that pore water salinity is the main factor controlling wetland dynamics (e.g., Alongi et al., 2000; Baltzer, 1975; Snedaker, 1982), and that salinity itself is regulated by rainfall, river water discharge, energy flow, tidal water salinity and inundation frequency (e.g., Cohen and Lara, 2003; Cohen et al., 2005a, 2008, 2009; Lara and Cohen, 2006), changes in soil salinity gradients have been driving wetland displacement (e.g., Cohen et al., 2008, 2009; Lara and Cohen, 2006).

3. Methods

3.1. Sampling sites and sample processing

Fieldwork was undertaken in June 2007, during the rainy season. Sediment cores LA-A (S00°35′52.1″/W49°08′35.2″), LA-B (S00°35′54.0″/W49° 09′49.9″), and LA-D (S00°43′40.9″/W49°10′00.4″) were taken from the bottom of Lake Arari under a water depth of 1.5–2.0 m. Another core (HP-A, S00°53′34.5″/W48°40′8.07″) was sampled 15 km from the margin of this lake, but within a drainage basin that feeds the lake (Fig. 1). The distribution of sediment cores in the study site is fundamental to verify the spatial representativeness of the pollen records in the lake bottom, and its capacity to record vegetation changes. Sediment cores were collected using a "Russian" sampler and their geographical positions were determined by GPS. The cores were submitted to X-rays to identify internal structures. Sediment color was described using a Munsell soil chart. Sediment grain size distribution following Wentworth (1922), with sand (2–0.0625 mm), silt (62.5–3.9 μm) and clay fraction (3.9–0.12 μm) was analyzed by laser diffraction in a Laser Particle Size SHIMADZU SALD 3101 and graphics were obtained using the SysGran Program (Camargo, 1999).

For pollen analyses, 1 cm^3 samples were taken at 2.5 cm intervals along the cores. Preparation followed standard pollen analytical techniques including acetolysis (Faegri and Iversen, 1989). Most pollen types were identified based on published morphological descriptions (Roubik and Moreno, 1991; Herrera and Urrego, 1996; Colinvaux et al., 1999) and the pollen reference collection held at the Laboratory of Coastal Dynamics (Federal University of Pará). A minimum of 300 pollen grains were counted for each sample. In specific depths, 100–200 grains were counted. Microfossils consisting of spores, algae and some fungal spores were also counted, but not included in the sum. The TILIA software package was used for calculations, and CONISS and TILIAGRAPH for the cluster analysis of pollen taxa and to plot the pollen diagrams (Grimm, 1987).

Eight subsamples of ~2 g each were used for radiocarbon dating (Table 1). Sediment samples were physically treated by removing roots and vegetation fragments under the microscope. The residual material was then chemically treated with 2% HCl at 60 °C during 4 h, washed with distilled water until neutral pH and dried (50 °C),

Table 1
Radiocarbon ages (AMS) from Lake Arari (LA) and the herbaceous plain (HP and S). Radiocarbon ages are presented in conventional yr B.P. and in cal. yr BP (±2σ), obtained with software package Calib 6.0 and the Intcal09 curve (Reimer et al., 2004).

Sample	Lab. number	Depth (cm)	Radiocarbon age (yr B.P.)	2-Sigma calibration[a] (cal yr B.P.)
LA-A	KIA34339	27	2010 ± 25	2005–1891
LA-A	KIA34340	62	3525 ± 30	3884–3706
LA-B	KIA34341	33	660 ± 25	670–632
LA-B	KIA34342	82	4020 ± 25	4530–4423
LA-D	UGAMS 6999	20	2160 ± 25	2306–2234
LA-D	KIA34344	30	5145 ± 25	5944–5888
LA-D	KIA34345	80	6335 ± 35	7328–7168
HP-A	KIA28165	32	635 ± 20	660–626
S1[b]	KIA28167	45	525 ± 35	564–504
S2[b]	KIA28168	28	540 ± 30	562–512

[a] Calibration Reimer et al. (2004).
[b] Cohen et al. (2008).

in order to remove any younger organic fractions (fulvic/humic acids) and carbonates. The sediments' organic matter was taken for Accelerator Mass Spectrometer (AMS) radiocarbon dating, performed at the Leibniz Laboratory of Isotopic Research at the Christian Albrechts University in Kiel (Germany) and the Center for Applied Isotope Studies at the University of Georgia (USA). Radiocarbon ages are presented in conventional yr B.P. and in cal. yr BP ($\pm 2\sigma$), obtained using the Calib 6.0 software and Intcal09 curve (Reimer et al., 2004).

4. Results

4.1. Radiocarbon dates and sedimentation rates

The dates are shown in Table 1 and range from 660–626 cal. yr BP to 7328–7168 cal. yr BP, and no age inversions were observed. Sedimentation rates were based on the ratio between depth intervals (mm) and the mean time range. The calculated sedimentation rates for the Lake Arari core are between 0.03 and 0.47 mm/yr. Core LA-A presents rates of 0.2 (62–27 cm) and 0.13 mm/yr (27–0 cm), while core LA-B shows rates of 0.13 (82–33 cm) and 0.47 mm/yr (33–0 cm). Core LA-D exhibits rates of ~0.37 mm/yr (80–30 cm) and relatively lower rates of ~0.03 mm/yr (30–20 cm) and 0.09 mm/yr (20–0 cm). Rates in the herbaceous plain were calculated to 0.46 (HP-A), 0.8 (S1 core, Cohen et al., 2008) and 0.5 mm/yr (S2 core, Cohen et al., 2008).

4.2. Facies description

4.2.1. LA-A

The sediments studied here include mostly dark gray and light brown, either muddy or sandy silt that is locally interbedded with fine-grained sand (Fig. 2). These deposits are massive, parallel laminated or heterolithic bedded (mostly wavy).

The base of core LA-A (62–45 cm, 3884–3706 cal. yr BP until ~2800 cal. yr BP) presents a transition from light gray muddy silt (8% sand, 71% silt, 21% mud) with discontinuous lenses of fine-grained sand to muddy silt (4% sand, 71% silt, 25% mud) with thin parallel laminae of fine-grained sand. The 45–35 cm interval (~2800–~2300 cal. yr BP) exhibits greenish gray sandy silt (29% sand, 55 silt, 16 mud) layers interbedded with fine-grained sand forming wavy structures and filling the upper portion of this section is a light brown massive muddy silt (5% sand, 72 silt, 23 mud). The 35–20 cm interval (~2300–~1600 cal. yr BP) exhibits a gradual transition, with massive muddy silt that grades upward into parallel laminated muddy silt (5% sand, 70% silt, 25% mud). Parallel laminated muddy silt between 30 and 20 cm gives rise upward to massive muddy silt (8% sand, 69 silt, 22 mud) that grades progressively into massive sandy silt (20% sand, 65% silt, 15% mud).

4.2.2. LA-B

Core LA-B between 82 and 72.5 cm (4530–4423 cal. yr BP until ~3700 cal. yr BP), displays light gray muddy silt (17% sand, 64% silt, 19% mud) with parallel lamination. Wavy heterolithic deposits occur between 72.5 and 67.5 cm. The 67.5–20 cm (~3300–~350 cal. yr BP) interval is marked by the grain size gradient along the muddy silt with thin parallel lamination of fine-grained sand. This trend continues to the upper edge of the core (20–0 cm, ~350 cal. yr BP–today) with massive muddy silt (2% sand, 73 silt, 25 mud).

4.2.3. LA-D

The base (80–60 cm, 7328–7168 cal. yr BP until ~6700 cal. yr BP) of the LA-D core presents light brown muddy silt (8% sand, 71% silt, 21% mud) with thin parallel lamination of fine-grained sand, while the 60–40 interval (~6700–~6200 cal. yr BP) exhibits reddish gray muddy silt (10% sand, 70% silt, 20% mud) and layers interbedded with fine-grained sand forming wavy structures. Between 40 and 20 cm (~6200 until 2306–2234 cal. yr BP) a greenish gray muddy silt (9% sand, 69 silt, 22 mud) is found with thin parallel lamination of fine-grained sand that gives rise upward to dark brown and dark gray massive muddy silt (12% sand, 66 silt, 22 mud).

4.2.4. HP-A

This sediment deposit (Fig. 1) exhibits homogeneous massive, dark gray, muddy silt (8% sand, 65% silt, 27% mud) sediments with organic matter along its entire depth of 32 cm. The base is marked by a rigid layer of white sandy material.

4.3. Pollen data

The first palynological study of Lake Arari was undertaken by Absy (1985), whom identified mainly *Alchornea*, Anacardiaceae, *Protium*, *Didymopanax*, *Mauritia*, Euphorbiaceae, and *Mabea* along a core of 5 m depth. In the present study a total of 38 pollen taxa were

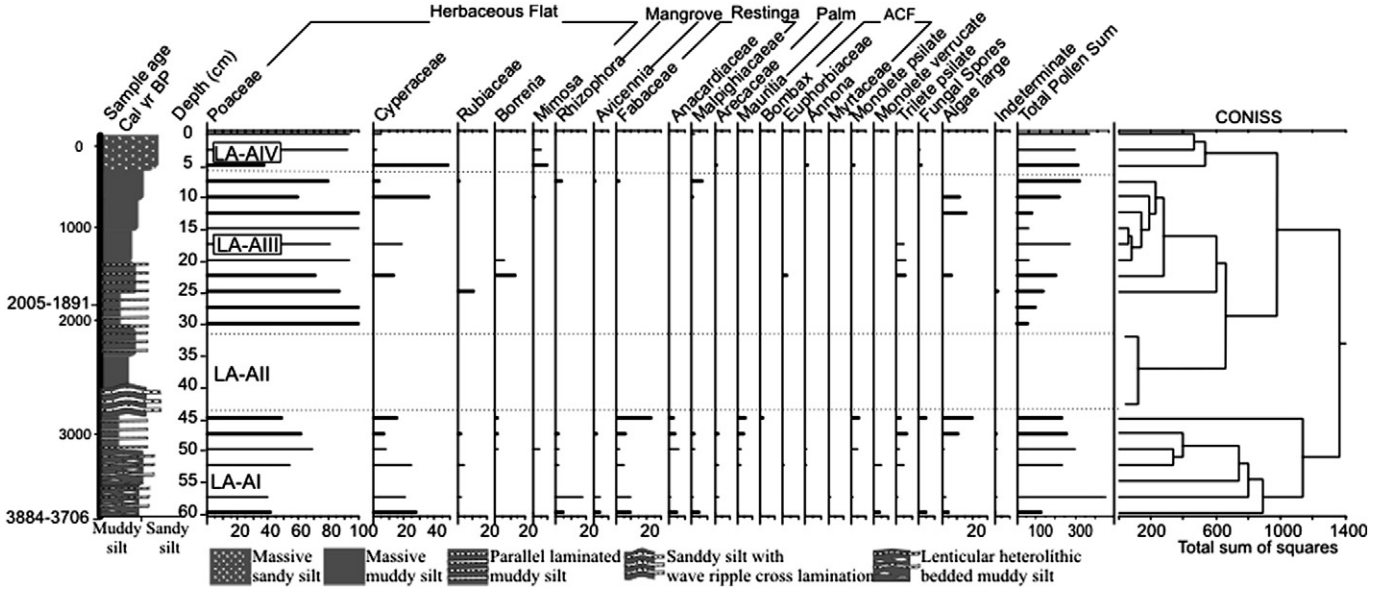

Fig. 2. Sediment core Lake Arari-A (LA-A). Sedimentary structure, sediment grain size, summary diagram of pollen proportion for different vegetation groups and proportions of the most frequent pollen taxa.

identified which, at the family level, represent 55% of the current vegetation distribution in and surrounding the drainage basin of Lake Arari.

Pollen diagrams (Figs. 2–5) show the most abundant pollen taxa and the sums for different ecological groups. Marked changes in pollen assemblages identified by cluster analysis (Coniss) allow the establishment of pollen zones, as described below.

4.3.1. LA-A core

This core, which is 63 cm long, contains herbaceous pollen (60–100%, Fig. 2), mainly represented by the Poaceae and Cyperaceae. Four pollen zones were distinguished: Zone LA-AI (62–45 cm, ~3884–3706 cal. yr BP until ~2800 cal. yr BP, 7 samples), Zone LA-AII (45–30 cm, ~2800–~2100 cal. yr BP, 6 samples), Zone LA-AIII (30–7.5 cm, ~2100–~500 cal. yr BP, 10 samples) and Zone LA-AIV (7.5–0 cm, ~540 cal. yr BP–modern, 3 samples).

In zone LA-AI, families Poaceae (40–72%) and Cyperaceae (10–30%) are the most common. Mangrove pollen has a low occurrence (0–22%), and is composed of *Rhizophora* (0–20%) and *Avicennia* (0–5%). *Restinga* vegetation also represented a low percentage of observed pollen (5–25%), and was predominantly characterized by Fabaceae (5–25%) and Anacardiaceae (0–7%). Low percentages of palm pollen (3–7%) were found, with the predominance of the *Mauritia* genus.

Zone LA-AII contains few pollen grains and spores (<80), thus it is not included in the pollen diagram. In the upper section of this zone, the percentage of herbaceous pollen increases upward. However, zone LA-AIII has a relatively low pollen content (100–200 pollen grains counted), predominately represented by herbaceous pollen of the Poaceae (65–100%) and Cyperaceae (0–40%).

Zone LA-AIV is characterized by a significant increase in pollen content (>300 pollen) with a predominance of Poaceae (40–90%) and Cyperaceae (5–50%) pollen.

4.3.2. LA-B core

Pollen diagram LA-B (Fig. 3) begins at a core depth of 82 cm, and is characterized by the predominance of herbaceous pollen (30–100%). Poaceae (0–100%) is the dominant family, followed by Cyperaceae (0–70%) and Asteraceae (0–50%).

Sediment core LA-B is composed of four zones (Fig. 3): LA-BI (82–77.5 cm, 4530–4423 cal. yr BP–~4100 cal. yr BP, 3 samples); LA-BII (77.5–65 cm; ~4100–~3100 cal. yr BP, 5 samples); LA-BIII (65–30 cm, ~3100–~600 cal. yr BP, 14 samples); and LA-BIV (30–0 cm, ~600 cal. yr BP–modern, 11 samples).

The LA-BI zone was found to contain 100–150 pollen grains. Herbaceous (~42%) and mangrove (10–40%) pollen dominates and is represented by the Poaceae (25–30%), Cyperaceae (10–15%), *Rhizophora* (0–15%) and *Avicennia* (10–30%). Zone LA-BII contains small amounts of pollen characterized by Poaceae (22–80%), Cyperaceae (0–70%) and Asteraceae (0–10%). The proportion of mangrove pollen decreases, and is represented only by *Avicennia* (0–25%).

Along zone LA-BIII, pollen content remains low, the proportion of herbaceous pollen (30–100%) increases, and is composed mainly of pollen from the Poaceae (30–100%), Cyperaceae (0–40%) and Asteraceae (0–35%), while mangrove pollen was not found.

4.3.3. LA-D core

This pollen record started at a core depth of 80 cm (Fig. 4), and consists of two pollen zones: 80–20 cm, 7328–7168 cal. yr BP until 2306–2234 cal. yr BP, 26 samples; and 20–0 cm, 2306–2234 cal. yr BP–modern, 7 samples. The main feature of this core is the relative importance of mangrove pollen (0–95%) in zone LA-DI and its reduced presence in zone LA-DII. In zone LA-DI, mangrove pollen represents a larger proportion of the total than herbaceous pollen (0–60%). This zone is dominated by *Rhizophora* (3–84%) and *Avicennia* (5–61%), while Poaceae (0–60%) and Cyperaceae (0–25%) occur at a lower percentage. Low pollen predominance (0–10%) of typical Amazon Coastal Forest-ACF taxa, such as Myrtaceae (0–10%), Anacardiaceae (0–5%), Acanthaceae (0–10%), Malpighiaceae (0–7%), *Sapium* sp. (0–5%), Bombacaceae (0–3%) and Euphorbiaceae (0–3%) occurs along the LA-DI zone.

Zone LA-DII contains a high proportion of herbaceous pollen (85–95%), represented by the Poaceae (75–92%), Cyperaceae (0–15%) and Asteraceae (0–5%). The proportion of mangrove pollen (2–15%) shows a significant decrease, and is characterized by *Rhizophora* (1–10%) and *Avicennia* (0–15%).

4.3.4. HP-A

In this core, only one pollen zone was preserved (32–0 cm, 660–626 cal. yr BP–modern, 14 samples). Herbaceous pollen (80–100%) prevails throughout this core (Fig. 5), and is mainly represented by the Poaceae (26–75%), Cyperaceae (10–50%) and Fabaceae (0–25%). A slight increase in *Rhizophora* pollen (0–20%) content occurs toward the bottom (5–27.5 cm), while pollen in the upper part is representative of the herbaceous vegetation that currently colonizes this area.

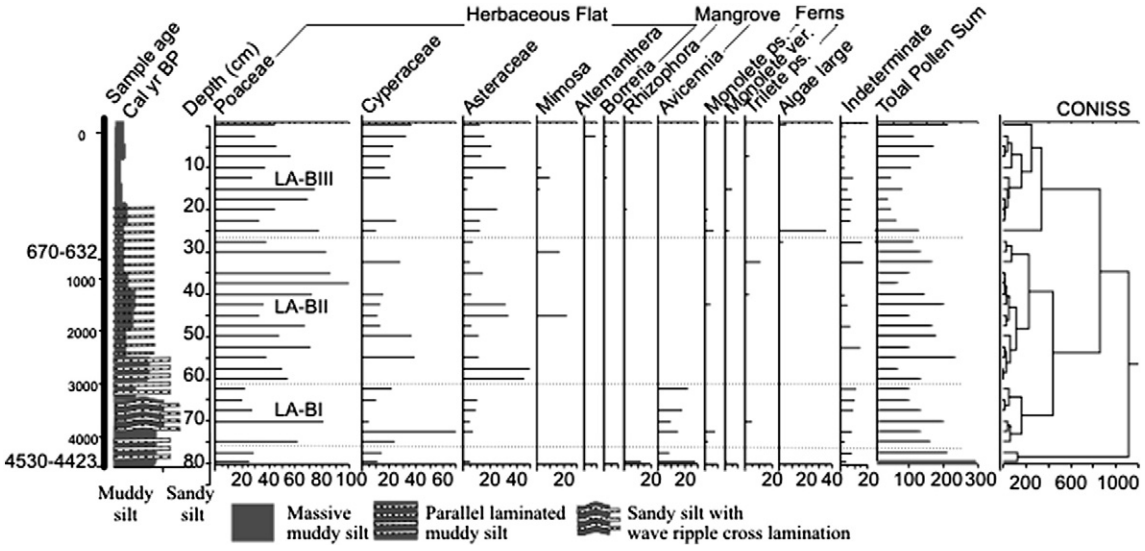

Fig. 3. Pollen records from Lake Arari-B (LA-B), sedimentary structure and grain size.

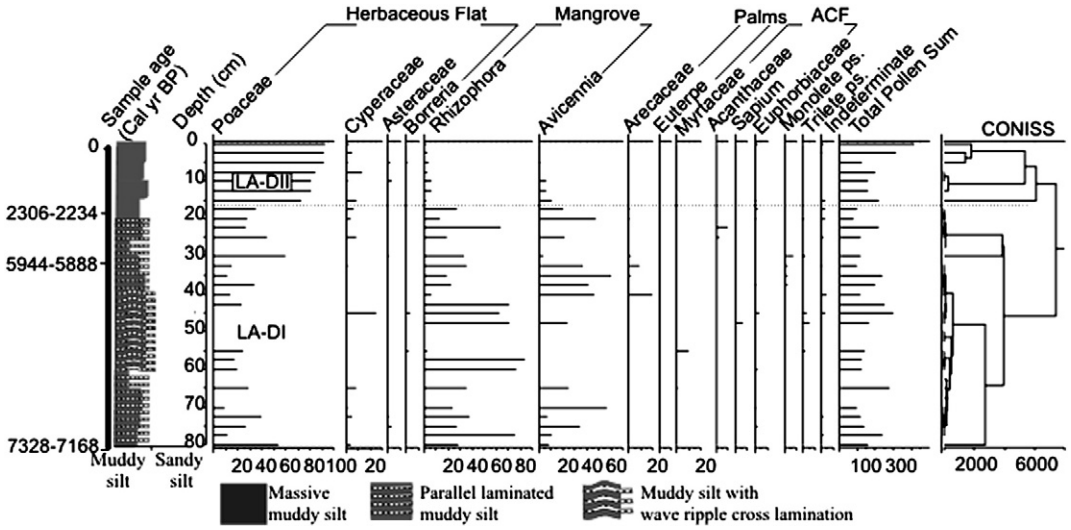

Fig. 4. Pollen records from Lake Arari-D (LA-D), sedimentary structure and grain size.

5. Discussion

According to Miranda et al. (2009), facies analysis, radiocarbon dating, $\delta^{13}C$, $\delta^{15}N$, and C/N of a 124 m long core from Marajó Island suggested the prevalence of estuarine conditions, with the dominance of fluvial deposition between 50,795 and 40,950 (±590) ^{14}C yr B.P., and a rise in relative sea-level that commenced between 39,079 (±1114) and 35,567 (±649) ^{14}C yr B.P. An overall transgression took place until 29,340 (±340) ^{14}C yr B.P., after which the relative sea-level dropped, favoring valley rejuvenation and incision. From this time up to 10,479 (±34) ^{14}C yr B.P., a rise in relative sea-level filled up the valley with estuarine deposits. After 10,479 (±34) ^{14}C yr B.P., the estuary was replaced by a lagoon.

5.1. Lagoon phase

According to our data, mangroves occurred in the drainage basin area of Lake Arari at least between 7328–7168 cal. yr BP and 2306–2234 cal. yr BP. Mangrove pollen accumulation occurred mainly during the formation of lamination and wave ripple structures. The greater concentration of mangrove pollen in the lower portions of core LA-D (7328–7168 and 2306–2234 cal. yr B.P.), core LA-B (4529–4423 cal. yr BP–~3400 cal. yr BP) and core LA-A (3794–3706 cal. yr BP–~2700 cal yr B.P.) suggests higher tidal water salinity on Marajó Island relative to the present.

In core LA-D, the wavy structures and parallel laminations (Fig. 4) suggest low energy flow with intermittent sand input during

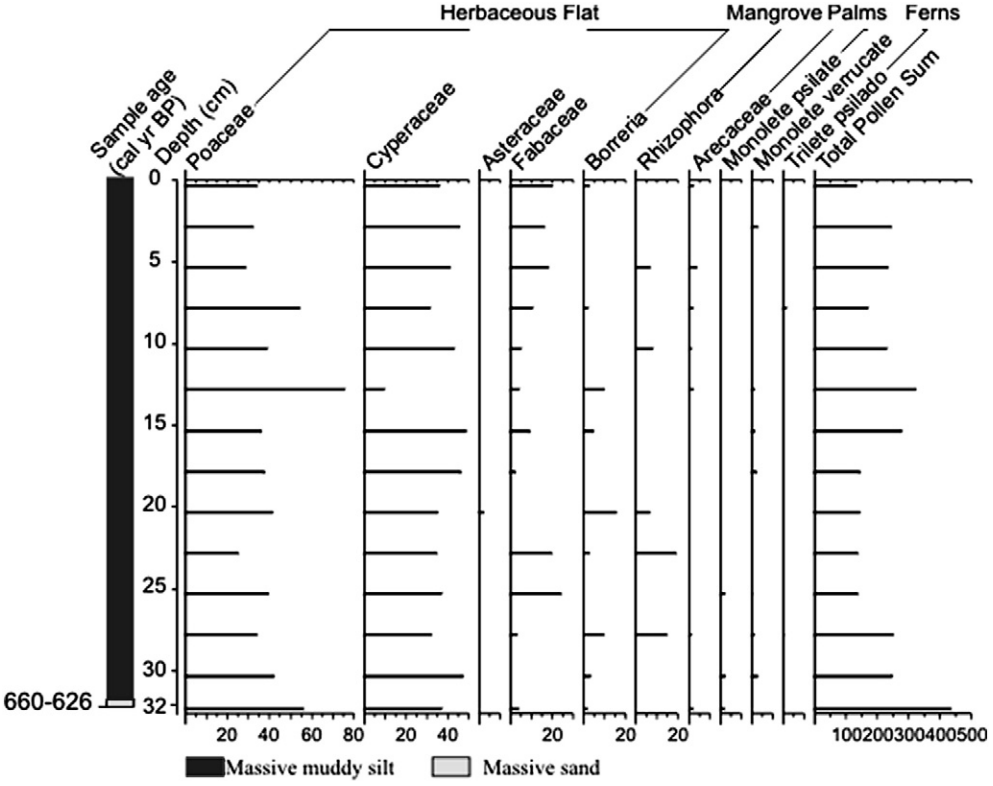

Fig. 5. Pollen records from the herbaceous plain (HP-A).

relatively higher energy flow that evolves to wave structures. In core LA-B, the thin parallel lamination of fine-grained sand and sandy silt with wave structures in the lower section (82–67.5 cm, 4529–4423 cal. yr BP–~3400 cal. yr BP) indicate low energy flow with episodic increases in energy flow (Fig. 3). The lower section (63–45 cm, 3884–3706 cal. yr BP–~2800 cal. yr BP) of core LA-A records episodic sand input and the deposition of laminated sand during muddy silt from suspension under low energy flow. Therefore, these sedimentary structures (lenticular, wavy ripples and parallel muddy silt/sandy silt deposits) could be attributed to a lagoon phase, when the effects of marine phenomena such as waves, wind-driven currents and tidal currents have a more evident impact on the distribution and reworking of sediments, and mangrove development.

5.2. Herbaceous phase

During the past 2306–2234 cal. yr BP, the absence of mangrove pollen and the prevalence of herbaceous pollen indicate similar vegetation to what is currently found at the site, which is typical of freshwater flooded environments. The mangrove/herbaceous transition phase occurs along sedimentary structures that suggest significant fluctuating low and relatively higher energy flow. The interval 67.5–33 cm of core LA-B (~3300 until 670–632 cal. yr BP) is characterized by a decrease in the energy flow evidenced by the grain size gradient along the muddy silt (Fig. 3), with thin parallel lamination of fine-grained sand and the presence of only herbaceous pollen. This trend continues to the upper section of the core with massive muddy silt and only herbaceous pollen.

Core LA-A records fluctuating low and relatively higher energy flow, with an equilibrium between muddy silt deposition from suspension and sandy silt from migrating ripples (45–35 cm, ~2800–~2300 cal. yr BP). No preserved pollen has been found in the 42.5–32.5 cm interval, probably due to the increase in sediment grain size. In the 35–20 cm interval (~2300–~1600 cal. yr BP), herbaceous pollen predominates which is preserved in parallel lamination of fine-grained sand in muddy silt. This indicates the deposition of muddy silt from suspension under very low energy flow and the sand laminations record episodic sand input during relatively higher freshwater energy flow.

Herbaceous pollen continues to be observed until the upper extremity of the LA-A core, but the pollen content increases, as does the sediment grain size which includes massive sandy silt. The absence of structures may suggest the absence of material transported by traction during sediment deposition, and the lack of mangrove pollen indicates a decrease in water salinity, which likely resulted from an increase in freshwater input to the lake.

At the study site – a lake system affected by seasonal influx of freshwater from its drainage system – the transition of sand laminations to massive structures likely reflects the change from fluctuating high and relatively lower energy flow, as the sheetfloods decelerate. These depositional differences may reflect variations in energy flow of surface runoff controlled by the drainage system of the lake.

Therefore, during the first phase (7328–7168 and 2306–2234 cal yr B.P.), sediment accumulation suggests a greater influence of wave and tidal currents than during the last phase (2306–2234 cal. yr BP–modern). This caused a change from a lagoon system to a lake with vegetation, and the sedimentation process was mainly controlled by its drainage system.

It is likely that during the late Holocene, mangroves in the drainage basin area of Lake Arari were not completely replaced by freshwater wetlands, since pollen data indicate the presence of mangroves between 700 and 500 cal. yr BP (Cohen et al., 2008). During this time interval, mangrove pollen was not found in cores LA-A, LA-B and LA-D. This likely reflects differences in sedimentation rates, with rates of 0.8–1.6 mm/yr for LA (Cohen et al., 2008) and of 0.03–0.47 mm/yr for LA-A, LA-B and LA-D.

The pollen profile of the herbaceous plain (HP-A) includes herbaceous pollen during the past 660–626 cal. yr BP, with pulses of *Rhizophora* pollen. A previous study (Cohen et al., 2008) recorded the predominance of herbaceous pollen in cores sampled from substratum nearly 15 km to the east of Lake Arari over the past 564–504 cal. yr BP (see S1 and S2 in Fig. 1).

Therefore, the integration of these data indicates the predominance of herbaceous vegetation during the past 2306–2234 cal. yr B.P. on the limit of the Lake Arari drainage basin, with some remaining *Rhizophora* indicating short phases with mangroves. The low *Rhizophora* pollen signal in the HP-A core may be attributed to the difference in the spatial representativeness of the vegetation between the cores sampled from the bottom of the lake and the herbaceous plain. The sediment of the HP-A core represents a relatively lower spatial representativeness, and thus they document the isolated presence of *Rhizophora* trees near the HP-A site.

5.3. Relationship between tectonic and vegetation changes

The sharp contact between forest and savanna occurs along a major NW–SE to NNW–SSE fault zone reactivated during the latest Quaternary (Rossetti et al., 2007a). A number of other studies have addressed the importance of tectonics in the latest Tertiary and Quaternary in Marajó Island (e.g., Rossetti and Valeriano, 2007). Following subsidence, eastern Marajó Island progressively stabilized, promoting a complex history of channel/bar establishment and abandonment (Rossetti et al., 2008). This tectonic subsidence favors seasonal flooding, making it unsuitable for forest growth. However, this area displays slightly convex-up, sinuous morphologies related to paleochannels, covered by forest.

Terra-firme lowland forests are expanding from west to east, preferentially occupying paleochannels and replacing savanna. Slack, running water during channel abandonment leads to the disappearance of varzea/gallery forest at channel margins. Long-abandoned channels sustain continuous terra-firme forests (Rossetti et al., 2010). Therefore, considering the influence of topography (Tuomisto et al., 1995; Vormisto et al., 2004), soil (Tuomisto and Ruokolainen, 1994) and geology (Räsänen et al., 1990; Van der Hammen et al., 1992) to explain species distribution, Rossetti et al. (2010) proposes that the history of drainage abandonment played crucial roles in tree growth in Marajó Island and in Amazonia region.

The coexistence on Marajó Island of periodically wet and permanently dry open areas covered with herbaceous vegetation, as well as “Terra Firme” vegetation, may be explained by vegetational succession (Whitmore, 2009), where herbaceous stands have been progressively replaced by “Terra Firme” vegetation following vegetation adaptation to the topography. According to Odum (1988), ecological succession includes changes in species structure and community processes over time, which cause changes in the physical environment of the community, competition interactions and coexistence at the population level.

Therefore, only physical processes may be used to explain the transition of Terra Firme to *várzea* vegetation in Marajó Island. However, these mechanisms cannot be used to explain the migration of certain wetlands (e.g., *várzea*/mangrove or herbs/mangrove) when the sediment surface is flooded by freshwater from river discharge or rainfall, because there is no saline source whereby salt may be concentrated in the sediment, and salinity is an essential physicochemical component for the survival of mangrove (e.g. Alongi et al., 2000; Baltzer, 1975; and Snedaker, 1982).

5.4. Relationship between tectonic control and relative sea-level

Mangroves have undergone significant changes in distribution as a result of sea-level fluctuations during the Holocene (e.g. Alongi, 2008; Behling et al., 2001a; Cohen et al., 2008). Tectonic movements can produce considerable subsidence or uplift of the coastal zone on a

local to regional scale that generate, jointly with other variables, relative sea-level changes (e.g., Emery and Aubrey, 1991; Möner, 1999). Tectonics may have controlled the evolution of the paleoestuary, and this has large implications for reconstructing the paleogeography and the history of relative sea-level changes in northern Brazil. Recent research (Rossetti et al., 2007a, 2008) revealed that the Marajó paleoestuary was active until the Pleistocene–Holocene boundary, when the island was detached from the mainland due to the reactivation of tectonic faults. Studies have demonstrated that this area has been affected by episodes of fault reactivation even during the Holocene (Rossetti and Valeriano, 2007; Rossetti et al., 2007a).

Facies analysis, radiocarbon dating, and isotopic data from Marajó Island indicate a progressive increase in marine inflow contribution during the Holocene, suggesting a maximum transgression. This interpretation is consistent with the overall rise in sea-level during the past interglacial period, when a barred lagoon system developed. The lagoon remained active in the Holocene, but the coastline prograded approximately 45 km northward; consequently, the lagoon was replaced by the present Lake Arari (Miranda et al., 2009).

However, this coastline progradation alone cannot justify the transition of mangrove/herbaceous vegetation from about 2306–2234 cal. yr BP on the drainage basin area of Lake Arari, because Marajó Island's current littoral is mainly colonized by freshwater wetlands. Therefore, it is likely that during lagoon development, not only was the center of Marajó Island more exposed to the sea, but water salinity was also greater than it is today.

5.5. Sea-level and climatic change

Greater water salinity in the lake during the mid-Holocene may be attributed to the rapid Atlantic sea-level rise during the early Holocene in South America (e.g., Angulo et al., 2008; Hesp et al., 2007; Rull et al., 1999; Suguio et al., 1985; Tomazelli, 1990) which produced a marine incursion into the continent, since the relative sea-level along the Pará littoral settled at the current level between 7000 and 5000 yr B.P. (Cohen et al., 2005a; Vedel et al., 2006). The stratigraphic framework of Lake Arari and nearby areas shows a transgressive phase taking place in the early to mid-late Holocene. Subsequently, there was a return to the more continental conditions that prevail today in the study area (Rossetti et al., 2008).

A sea-level rise alone was likely not sufficient to produce a rise in tidal water salinity and, consequently, a significant expansion of mangroves. Indeed, during the past 5000 years the sea-level did not show significant oscillations along the Pará littoral (Cohen et al., 2005a). Additionally, freshwater discharge from modern rivers near Marajó Island has been kept at low tidal water salinity (0–6‰). Consequently, mangroves are restricted to a few occurrences in northeastern Marajó Island (Cohen et al., 2008). It is thus likely that, between 7328–7168 cal. yr BP and 2306–2234 cal. yr BP, freshwater discharge from rivers was lower than it is today, and the post-glacial eustatic sea-level rise produced a rise in tidal water salinity.

The proposed relatively low freshwater discharge during 7328–7168 cal. yr BP and 2306–2234 cal. yr BP may be a consequence of the dry periods recorded in different parts of the Amazon region (Fig. 6). For example, $\delta^{13}C$ analysis of soil organic matter collected in forested and woody savanna areas from the coast of Maranhão indicates that from approximately 10,000 and 9000 yr B.P. to 4000 yr B.P., a woody savanna prevailed, likely reflecting a drier climate (Pessenda et al., 2004). From 4000–3000 yr B.P. to present, there was a moderate and progressive increase in arboreal vegetation in the southern Amazon basin, due to the return to more humid climate conditions, likely similar to the present day (Freitas, et al., 2001; Pessenda et al., 2004). Isotopic studies in the southern Brazilian Amazon region indicate a drier climate during the mid-Holocene, while the data reflects forest expansion associate to

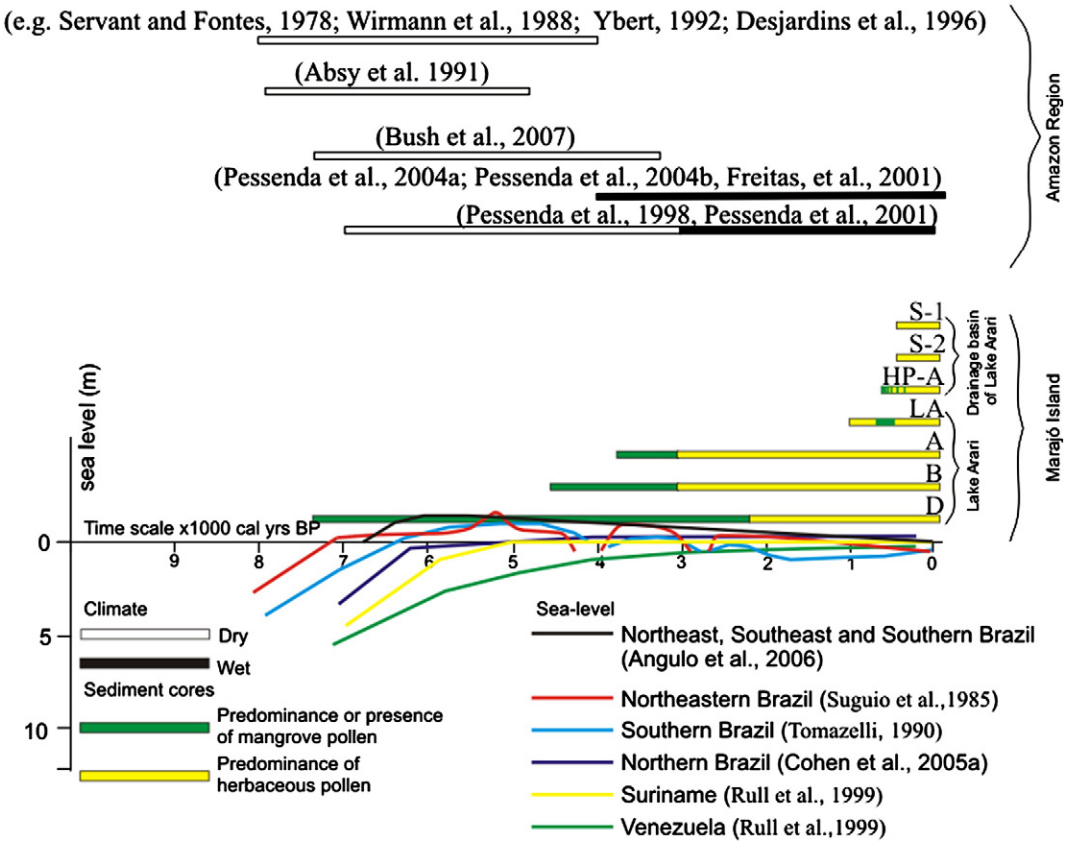

Fig. 6. Comparative diagram of climatic change records in the Amazon region, sea-level rise in eastern South America during the Holocene, and the pollen diagram from Lake Arari.

the wet period of the past 3000 years (Pessenda et al., 1998, 2001a). In the Colombian Amazon, drier early Holocene and wetter late Holocene conditions are also reported (Behling and Hooghiemstra, 2000). This trend is similar to other documented forest-to-savanna vegetation changes in the Amazon basin during the early and middle Holocene (Behling et al., 2001b; Desjardins et al., 1996; Pessenda et al., 2001b).

Paleoecological records from lakes in the Peruvian Amazon indicate a dry event from ~7200 yr B.P. until c. 3300 yr B.P. (Bush et al., 2007). Palynological and paleolimnological studies in eastern Amazonia have shown that savannas appeared, with the development of a drier climate, beginning 8000 years B.P., reaching a maximum distribution from 6000 to 5000 yr B.P. (Absy et al., 1991). Dry periods during 8000–4000 yr B.P. in areas close to and in the Amazon region have also been documented (e.g., Absy et al., 1991; Desjardins et al., 1996; Servant and Fontes, 1978; Wirmann et al., 1988).

6. Conclusion

Pollen preservation in sedimentary deposits from Lake Arari and its drainage basin suggests significant vegetation changes on Marajó Island during the mid and late-Holocene. Between 7328–7168 and 2306–2234 cal. yr BP, mangrove vegetation was more widely distributed than it is today on the island, while during the past 2306–2234 cal. yr BP herbaceous vegetation expanded. Sedimentary structures and pollen data suggest a lagoon system until ~2300 cal. yr BP. The current distribution of mangroves along the Pará littoral, the presence of mangrove pollen and sedimentary structures of the cores indicate a greater marine influence during the mid-Holocene than in the late-Holocene. This may be attributed to the association between the post-glacial eustatic sea-level rise and the dry period recorded in Amazonia during the early and mid-Holocene, followed by a wet phase over the past 2200 years.

Acknowledgments

This work was funded by CNPq (Project 562398/2008-2). The first and second authors hold a scholarship from CNPq (Process 140034/2007-2 and 302943/2008-0). The authors thank the members of the Laboratório de Ciências Ambientais — LCA (UENF-RJ) and Dr. Carlos Eduardo Rezende for their support with determining sediment grain size.

Appendix A. Supplementary data

Supplementary data to this article can be found online at doi:10.1016/j.revpalbo.2011.09.008.

References

Absy, M.L., 1985. Palinology of Amazonia: the history of the forests as revealed by the palynological record. In: Prance, G.T., Lovejoy, T.E. (Eds.), Amazonia. Pergamon Press, Oxford, United Kingdom. 442 pp.

Absy, M.L., Clief, A., Fournier, M., Martin, L., Servant, M., Siffeddine, A., Silva, F.D., Soubiès, F., Suguio, K.T., Van der Hammen, T., 1991. Mise em évidence de Quatre phases d'ouverture de la forêt dense dans le sud-est de L'Amazonie au cours des 60,000 dernières années. Première comparaison avec d'autres régions tropicales. Comptes Rendus Academie des Sciences Paris 312, 673–678.

Alongi, D.M., 2008. Mangrove forests: resilience, protection from tsunamis, and responses to global climate change. Estuarine, Coastal and Shelf Science 76, 1–13.

Alongi, D.M., Tirendi, F., Clough, B.F., 2000. Below-ground decomposition of organic matter in forests of the mangrove *Rhizophora stylosa* and *Avicennia marina* along the arid coast of Western Australia. Aquatic Botany 68, 97–122.

Amarasekera, K.N., Lee, R.F., Williams, E.R., Eltahir, E.A.B., 1997. ENSO and the natural variability in the flow of tropical rivers. Journal of Hydrology 200, 24–39.

Angulo, R.J., de Souza, M.C., Assine, M.L., Pessenda, L.C.R., Disaró, S.T., 2008. Chronostratigraphy and radiocarbon age inversion in the Holocene regressive barrier of Paraná, southern Brazil. Marine Geology 252, 111–119.

Baltzer, F., 1975. Solution of silica and formation of quartz and smectite in mangrove swamps and adjacent hypersaline marsh environments. Proceedings of the International Symposium on Biology and Management of Mangroves, Univ. Florida, pp. 482–498.

Behling, H., Hooghiemstra, H., 2000. Holocene Amazon rainforest–savanna dynamics and climatic implications: high-resolution pollen record from Laguna Loma Linda in eastern Colombia. Journal of Quaternary Science 15, 687–695.

Behling, H., Cohen, M.C.L., Lara, R.J., 2001a. Studies on Holocene mangrove ecosystem dynamics of the Bragança Peninsula in north-eastern Pará, Brazil. Palaeogeography, Palaeoclimatology, Palaeoecology 167, 225–242.

Behling, H., Keim, G., Irion, G., Junk, W., Nunes de Mello, J., 2001b. Holocene environmental changes in the Central Amazon Basin inferred from Lago Calado (Brazil). Palaeogeography, Palaeoclimatology, Palaeoecology 173, 87–101.

Behling, H., Cohen, M.C.L., Lara, R.J., 2004. Late Holocene mangrove dynamics of the Marajó Island in northern Brazil. Vegetation History and Archaeobotany 13, 73–80.

Blasco, F., Saenger, P., Janodet, E., 1996. Mangroves as indicators of coastal change. Catena 27, 167–178.

Bush, M.B., Silman, M.R., Listopad, C.M.C.S., 2007. A regional study of Holocene climate change and human occupation in Peruvian Amazonia. Journal of Biogeography 34, 1342–1356.

Camargo, M.G., 1999. SYSGRAN for Windows: Granulometric Analyses System. Pontal do Sul. Paraná. Brasil.

Cohen, M.C.L., Lara, R.J., 2003. Temporal changes of mangrove vegetation boundaries in Amazonia: application of GIS and remote sensing techniques. Wetlands Ecology and Management 11, 223–231.

Cohen, M.C.L., Behling, H., Lara, R.J., 2005a. Amazonian mangrove dynamics during the last millennium: the relative sea-level and the little ice age. Review of Palaeobotany and Palynology 136, 93–108.

Cohen, M.C.L., Souza Filho, P.W., Lara, R.L., Behling, H., Angulo, R., 2005b. A model of Holocene mangrove development and relative sea-level changes on the Bragança Peninsula (northern Brazil). Wetlands Ecology and Management 13, 433–443.

Cohen, M.C.L., Lara, R.J., Smith, C.B., Angelica, R.S., Dias, B.S., Pequeno, T., 2008. Wetland dynamics of Marajó Island, northern Brazil during the last 1000 years. Catena 76, 70–77.

Cohen, M.C.L., Behling, H., Lara, R.J., Smith, C.B., Matos, H.R.S., Vedel, V., 2009. Impact of sea-level and climatic changes on the Amazon coastal wetlands during the late Holocene. Vegetation History and Archaeobotany 18, 1–15.

Colinvaux, P.A., De Oliveira, P.E., Patiño, J.E.M., 1999. Amazon Pollen Manual and Atlas. Hardwood, Amsterdam.

Desjardins, T., Filho, A.C., Mariotti, A., Chauvel, A., Girardin, C., 1996. Changes of the forest–savanna boundary in Brazilian Amazonia during the Holocene as revealed by soil organic carbon isotope ratios. Oecologia 108, 749–756.

Duke, N.C., Ball, M.C., Ellison, J.C., 1998. Factors influencing biodiversity and distributional gradients in mangroves. Global Ecology and Biogeography Letters 7, 27–47.

Eisma, D., Augustinus, P.G.E.F., Alexander, C., 1991. Recent and subrecent changes in the dispersal of Amazon mud. Netherlands Journal of Sea Research 28, 181–192.

Emery, K.O., Aubrey, D.G., 1991. Sea Levels, Land Levels, and Tide Gauges. Springer Verlag, New York.

Faegri, K., Iversen, J., 1989. Textbook of Pollen Analysis, Fourth ed. Wiley, J., Sons, X. New York.

Fairbridge, R.W., 1962. World sea-levels and climatic changes. Quaternaria 6, 111–134.

Freitas, H.A., Pessenda, L.C.R., Aravena, R., Gouveia, S.E.M., Ribeiro, A.S., Boulet, R., 2001. Late Quaternary vegetation dynamics in the Southern Amazon Basin inferred from carbon isotopes in soil organic matter. Quaternary Research 55, 39–46.

Furukawa, K., Wolanski, E., 1996. Sedimentation in mangrove forests. Mangrove and Salt Marshes 1, 3–10.

Gonçalves-Alvim, S.J., Vaz dos Santos, M.C.F., Fernandes, G.W., 2001. Leaf gall abundance on *Avicennia germinans* (Avicenniaceae) along an interstitial salinity gradient. Biotropica 33, 69–77.

Grimm, E.C., 1987. CONISS: a Fortran 77 program for stratigraphically constrained cluster analysis by the method of the incremental sum of squares. Pergamon Journals 13, 13–35.

Hait, A.H., Behling, H., 2009. Holocene mangrove and coastal environmental changes in the western Ganga–Brahmaputra Delta, India. Vegetation History and Archaeobotany 18, 159–169.

Herrera, L.F., Urrego, L.E., 1996. Atlas de polen de plantas útiles y cultivadas de la Amazonia colombiana (Pollen atlas of useful and cultivated plants in the Colombian Amazon region). Estudios en la Amazonia Colombiana XI, Tropenbos–Colombia, Bogotá.

Hesp, P.A., Dillenburg, S.R., Barboza, E.G., Clerot, L.C.P., Tomazelli, L.J., Zouain, R.N.A., 2007. Morphology of the Itapeva to Tramandai transgressive dunefield barrier system and mid- to late Holocene sea level change. Earth Surface Processes and Landforms 32, 407–414.

Hutchings, P., Saenger, P., 1987. Ecology of Mangroves. Queensland University Press, St. Lucia.

IDESP, Institute of Social and Economic development of the Pará, 1974. Integrated Studies of Marajó Island. Belém. 333 pp.

Kjerfve, B., Lacerda, L.D., 1993. Mangroves of Brazil. In: Lacerda, L.D. (Ed.), Conservation and Sustainable Utilization of Mangrove Forests in Latin America and Africa Regions. Part I — Latin America. ITTO/International Society for Mangrove Ecosystems, Okinawa, Japan, pp. 245–272.

Krauss, K.W., Lovelock, C.E., McKee, K.L., López-Hoffman, L., Ewe, S.M.L., Sousa, W.P., 2008. Environmental drivers in mangrove establishment and early development: a review. Aquatic Botany 89, 105–127.

Lara, R.J., Cohen, M.C.L., 2006. Sediment porewater salinity and mangrove vegetation height in Bragança, North Brazil: an ecohydrology-based empirical model. Wetlands Ecology and Management 14, 349–358.

Lara, R.J., Cohen, M.C.L., 2009. Palaeolimnological studies and ancient maps confirm secular climate fluctuations in Amazonia. Climatic Change 94, 399–408.

Marengo, J. A., Tomasella, J., Soares, W. R., Alves, L. M., Nobre, C.A., in press. Extreme climatic events in the Amazon basin. Theoretical and Applied Climatology. DOI 10.1007/s00704-011-0465-1.
Martelli, L.R., Rossetti, D.F., Albuquerque, P.G., Valeriano, M.M., 2009. Applying SRTM digital elevation model to unravel Quaternary drainage in forested areas of Northeastern Amazonia. Computers & Geosciences 35, 2331–2337.
Maslin, M.A., Burns, S.J., 2000. Reconstruction of the Amazon Basin effective moisture availability over the past 14,000 years. Science 290, 2285–2287.
Miranda, M.C.C., Rossetti, D.F., Pessenda, L.C.R., 2009. Quaternary paleoenvironments and relative sea-level changes in Marajó Island (Northern Brazil): facies, $\delta^{13}C$, $\delta^{15}N$ and CN. Palaeogeography, Palaeoclimatology, Palaeoecology 282, 19–31.
Möner, N.A., 1999. Sea level and climate: rapid regressions at local warm phases. Quaternary International 60, 75–82.
Mörner, N.A., 1996. Global change and interaction of earth rotation, ocean circulation and paleoclimate. Anais da Academia Brasileira de Ciências 68, 77–94.
Odum, E.P., 1988. Ecologia. Rio de Janeiro, Ed. Guanabara Koogan. 434 pp.
Pessenda, L.C.R., Gouveia, S.E.M., Aravena, R., Gomes, B.M., Boulet, R., Ribeiro, A.S., 1998. ^{14}C dating and stable carbon isotopes of soil organic matter in Forest–savana boundary areas in Southern Brazilian Amazon Region. Radiocarbon 40, 1013–1022.
Pessenda, L.C.R., Gouveia, S.E.M., Aravena, R., 2001a. Radiocarbon dating of total soil organic matter and humin fraction and its comparison with ^{14}C ages of fossil charcoal. Radiocarbon 43, 595–601.
Pessenda, L.C.R., Boulet, R., Aravena, R., Rosolen, V., Gouveia, S.E.M., Ribeiro, A.S., Lamote, M., 2001b. Origin and dynamics of soil organic matter and vegetation changes during the Holocene in a forest–savanna transition zone, Brazilian Amazon region. The Holocene 11, 250–254.
Pessenda, L.C.R., Ribeiro, A.S., Gouveia, S.E.M., Aravena, R., Boulet, R., Bendassoli, J.A., 2004. Vegetation dynamics during the late Pleistocene in the Barreirinhas region, Maranhão State, northeastern Brazil, based on carbon isotopes in soil organic matter. Quaternary Research 62, 183–193.
Pujos, M., Latouche, C., Maillet, N., 1996. Late quaternary paleoceanography of the French Guiana continental shelf: clay-mineral evidence. Oceanologica Acta 19, 477–487.
Räsänen, M.E., Salo, J.S., Jungner, H., Romero-Pittman, L., 1990. Evolution of the Western Amazon lowland relief: impact of Andean foreland dynamics. Terra Nova 2, 320–332.
Reimer, P.J., Baillie, M.G.L., Bard, E., Bayliss, A., Beck, J.W., Bertrand, C., Blackwell, P.J., Buck, C.E., Burr, G., Cutler, K.B., Damon, P.E., Edwards, R.L., Fairbanks, R.G., Friedrich, M., Guilderson, T.P., Hughen, K.A., Kromer, B., McCormac, F.G., Manning, S., Bronk Ramsey, C., Reimer, R.W., Remmele, S., Southon, J.R., Stuiver, M., Talamo, S., Taylor, F.W., van der Plicht, J., Weyhenmeyer, C.E., 2004. Radiocarbon 46, 1029–1058.
Rossetti, D.F., Valeriano, M.M., 2007. Evolution of the lowest Amazon basin modeled from the integration of geological and SRTM topographic data. Catena 70, 253–265.
Rossetti, D.F., Goes, A.M., Valeriano, M.M., Miranda, M.C.C., 2007a. Quaternary tectonics in a passive margin: Marajo Island, northern Brazil. Journal of Quaternary Science 22, 1–15.
Rossetti, D.F., Valeriano, M.M., Thales, M., 2007b. An abandoned estuary within Marajó Island: implications for Late Quaternary paleogeography of northern Brazil. Estuaries and Coasts 30, 813–826.
Rossetti, D.F., Valeriano, M.M., Goes, A.M., Thales, M., 2008. Palaeodrainage on Marajó Island, northern Brasil, in relation to Holocene relative sea-level dynamics. The Holocene 18, 01–12.
Rossetti, D.F., Almeida, S., Amaral, D.D., Lima, C.M., Pessenda, L.C.R., 2010. Coexistence of forest and savanna in an Amazonian area from a geological perspective. Journal of Vegetation Science 21, 120–132.
Roubik, D.W., Moreno, J.E., 1991. Pollen and Spores of Barro Colorado Island, vol. 36. Missouri Botanical Garden, St. Louis.
Rull, V., Vegas-Vilarrubia, T., Espinoza, N.P., 1999. Palynological record of an early-mid Holocene mangrove in eastern Venezuela: implications for sea-level rise and disturbance history. Journal of Coastal Research 15, 496–504.
Santos, M.L.S., Medeiros, C., Muniz, K., Feitosa, F.A.N., Schwamborn, R., Macedo, S.J., 2008. Influence of the Amazon and Pará Rivers on water composition and phytoplankton biomass on the adjacent shelf. Journal of Coastal Research 24, 585–593.
Servant, M., Fontes, J.C., 1978. Les lacs quaternaries des hauts plateaux des Andes boliviennes. Premieres interpretation paleoclimatiques. Cahiers de L'ORSTOM Serie Geologie 10, 9–23.
Snedaker, S.C., 1982. Mangrove species zonation: why? In: Sen, D.N., Rajpurohit, K.S. (Eds.), Contributions to the Ecology of Halophytes, Tasks for Vegetation Science, vol 2. Junk, The Hague, pp. 111–125.
Stevens, P.W., Fox, S.L., Montague, C.L., 2006. The interplay between mangroves and saltmarshes at the transition between temperate and subtropical climate in Florida. Wetlands Ecology and Management 14, 435–444.
Stuart, S.A., Choat, B., Martin, K.C., Holbrook, N.M., Ball, M.C., 2007. The role of freezing in setting the latitudinal limits of mangrove forests. New Phytologist 173, 576–583.
Suguio, K., Martin, L., Bittencourt, A.C.S.P., Dominguez, J.M.L., Flexor, J.M., Azevedo, A.E.G., 1985. Flutuações do nível relativo do mar durante o Quaternário superior ao longo do litoral brasileiro e suas implicações na sedimentação costeira. Revista Brasileira de Geociências 15, 273–286.
Toledo, M.B., Bush, M.B., 2007. A mid-Holocene environmental change in Amazonian savannas. Journal of Biogeography 34, 1313–1326.
Toledo, M.B., Bush, M.B., 2008. Vegetation and hydrology changes in Eastern Amazonia inferred from a pollen record. Anais da Academia Brasileira de Ciencias 80, 191–203.
Tomazelli, L.J., 1990. Contribuição ao Estudo dos Sistemas Deposicionais Holocênicos do Nordeste da Província Costeira do Rio Grande do Sul, com Ênfase no Sistema Eólico, Ph.D. Thesis. Universidade Federal do Rio Grande do Sul, Porto Alegre.
Tuomisto, H., Ruokolainen, K., 1994. Distribution of Pteridophyta and Melastomataceae along an edaphic gradient in an Amazonian rain forest. Journal of Vegetation Science 5, 25–34.
Tuomisto, H., Ruokolainen, K., Kalliola, R., Linna, A., Danjoy, W., Rodriguez, Z., 1995. Dissecting Amazonian biodiversity. Science 269, 63–66.
Van der Hammen, T., Duivenvoorden, J.F., Lips, J.M., Urrego, L.E., Espejo, N., 1992. The late Quaternary of themiddle Caquetá area (Colombian Amazonia). Journal of Quaternary Sciences 7, 45–55.
Vedel, V., Behling, H., Cohen, M.C.L., Lara, R.J., 2006. Holocene mangrove dynamics and sea-level changes in northern Brazil, inferences from the Taperebal core in northeastern Pará State. Vegetation History and Archaeobotany 15, 115–123.
Versteegh, G.J.M., Schefuß, E., Dupont, L., Marret, F., Sinninghe Damste, J.S., Jansen, J.H.F., 2004. Taraxerol and *Rhizophora* pollen as proxies for tracking past mangrove ecosystems. Geochimica et Cosmochimica Acta 68, 411–422.
Vormisto, J., Tuomisto, H., Oksanen, T., 2004. Palm distribution patterns in Amazonian rainforests: what is the role of topographic variation? Journal of Vegetation Science 15, 485–494.
Wentworth, C.K., 1922. A scale of grade and class terms for clastic sediments. Journal of Geology 30, 377–392.
Whitmore, T.C., 2009. An Introduction to Tropical Rain Forests. Oxford University Press, New York. 251 pp.
Wirmann, D., Mourguiart, P., De Oliveira, L., 1988. Holocene sedimentology and ostracods repartition in Lake Titicaca. Paleohydrological interpretation. Quaternary of South America and the Antartic Peninsula 6, 89–127.
Wolanski, E., Mazda, Y., King, B., Gay, S., 1990. Dynamics, flushing and trapping in Hinchinbrook Channel, a giant mangrove swamp, Australia. Estuarine, Coastal and Shelf Science 31, 555–579.